Environ Sci Pollut Res (2016) 23:12535–12553
DOI 10.1007/s11356-016-6317-x

On the geotechnical characterisation of the polluted submarine sediments from Taranto

Claudia Vitone[1] · Antonio Federico[1] · Alexander M. Puzrin[2] · Michael Ploetze[2] · Elettra Carrassi[1] · Francesco Todaro[1]

Received: 10 May 2015 / Accepted: 16 February 2016 / Published online: 24 February 2016

Abstract This paper reports the results of the first geomechanical laboratory experiments carried out on the polluted submarine clayey sediments of the Mar Piccolo in Taranto (South of Italy). The study had to face with extreme difficulties for the very soft consistency of the sediments and the contaminants. The mineralogy, composition and physical properties of the sediments were analysed, along with their compression and shearing behaviour. The investigation involved sediments up to about 20 m below the seafloor, along three vertical profiles in the most polluted area of the Mar Piccolo, facing the Italian Navy Arsenal. The experimental results were used to derive a preliminary geotechnical model of the site, necessary for the selection and design of the most sustainable in situ mitigation solutions. Moreover, the experimental data reveal that the clayey sediments of the most polluted top layer do not follow the classical geotechnical correlations for normally consolidated deposits. This seems to open interesting perspectives about the effects of pollutants on the geotechnical behaviour of the investigated sediments.

Keywords Submarine sediments · Geotechnical characterisation · Contaminated soils · Mechanical behaviour

Responsible editor: Philippe Garrigues

✉ Claudia Vitone
claudia.vitone@poliba.it

1 Politecnico di Bari, Bari, Italy

2 Institute for Geotechnical Engineering, ETH Zurich, Zürich, Switzerland

Introduction and scope

The city of Taranto in the south of Italy is one of the areas declared as “at high risk of environmental crisis” by the national government (Italian Law n. 349 1986) because it represents one of the most complex industrial sites in Europe, located near urban areas of high population density. All the industrial activities are responsible for the high environmental contamination, mainly due to heavy metals and organic pollutants. This is why Taranto has been recently included into the list of polluted Sites of National Interest (SIN) by the Italian Law n. 426 1998, for which the environmental remediation has been identified as a national priority (Ministerial Decree n. 468 2002).

The Mar Piccolo (literally, Small Sea) basin is located in the northern area of Taranto city (Fig. 1a). It is a semi-enclosed shallow coastal basin (total surface of 20.72 km^2) with lagoon features, divided into the so-called first and second bosom. It is presently connected with the open sea (Mar Grande in the Ionian Sea) by two channels, the Navigabile Channel and the Porta Napoli Channel (Fig. 1a). As a consequence of the heavy industrialisation experienced by the Taranto city during the last 50 years, the complex ecosystem of the Mar Piccolo area started exhibiting unconfutable signs of environmental pollution enhanced by several uncontrolled discharged sewages, the activities of the Arsenal of the main naval base of the Italian Navy and the fishing-boat fleet. A number of researchers (e.g. Lerario et al. 2003; ICRAM-APAT 2007; Cardellicchio et al. 2007, 2009; ISPRA 2010; Petronio et al. 2012; Di Leo et al. 2013) have shown that also the submarine sediments in the Mar Piccolo contain high concentrations of heavy metals (e.g. Hg, Pb, Cd, Cu and Zn) and organic pollutants (PCBs, PAHs and dioxins).

This experimental research is part of the multidisciplinary studies that have been funded by the Regional Agency for

Fig. 1 **a** Gulf of Taranto and sampling area within the first bosom of Mar Piccolo; **b** location of the three boreholes (1I, 1L and 1M) and of the three samples taken by scuba divers (1I-M, 1L-M and 1M-M) within the "170-ha area"

Environmental Protection (ARPA-Puglia), and financially supported by specific national legislative procedures (Italian Law n. 129 2012), for a preliminary selection of sustainable strategies for the remediation and management of the Mar Piccolo environmental contamination. Among the different aspects involved in the environmental studies, i.e. sediments, water and biota, this paper focuses on submarine sediments and reports and implements the results of the first geotechnical investigation carried out in the Mar Piccolo (Federico and Vitone 2014). This up-to-date knowledge contributes to the definition of a site geotechnical model of reference for the selection, design, placement and management of the potential remedy approaches (e.g. Rolling 2000; Lee 2001; USEPA 2005).

In general, the transport of contaminants can be caused by mechanisms like molecular diffusion, pore water advection and bioturbation. Pore water advection from the sediment can be driven by two mechanisms: (i) submarine groundwater discharge and (ii) consolidation of contaminated sediment. The analysis of both these mechanisms requires the knowledge of the geotechnical properties of the sediments, together with that of the in situ chemical, hydrological, hydrogeological and geological conditions. Transport of metals from capped contaminated sediments due to submarine vertical flow from the artesian aquifer at the base has been studied by Liu et al. (2001), as an example of hydrogeological conditions that cause groundwater release through the seafloor.

However, for fine-grained contaminated sediments, like those present in the Mar Piccolo, the main mechanism of pore water advection is caused by the consolidation of the contaminated sediment. As the sediments are loaded (e.g. by the placement of a cap) or unloaded (e.g. by dredging operations), due to change of effective stress they will change in volume. Since the submarine sediments are soft saturated soils, their change in volume must be due to the water seepage and so the compression of the contaminated sediments is rather like squeezing contaminated water from a soft sponge of large pores. Since the contaminated water can seep to the capped surface but also towards natural drainage layers (if any), the knowledge of both the hydrogeological and geotechnical boundary conditions within the entire volume of soil interested by the remediation solution is necessary. The sufficient time for the water to seep through the soil to permit the volume change to occur is strictly dependant on the consolidation properties of the soil. In this respect, some researchers have highlighted the relevance of the knowledge of consolidation properties of the contaminated soils in order to predict the transport of contaminants by pore water advection. For example, Lenhart et al. (2009) performed tests of one-dimensional consolidation in the laboratory to simulate in situ fluxes using sediments contaminated by polychlorinated biphenyl, dredged from the Grand Calumet River in Gary, Indiana (USA). The tests were conducted both without a cap and using three capping materials (quartz sand, activated carbon and a proprietary organoclay). Eek et al. (2007) explored, instead, how different capping materials affect the metal concentration in pore water released from contaminated soft-silty clays from the Oslo harbour.

As remarked by USEPA (2005), another relevant geotechnical issue is the bearing capacity of the sediments for the cap stability. This has to be checked both immediately after placement (short term behaviour), i.e. before any excess pore water pressure due to the weight of the cap has dissipated, and in the long term, when the excess pore pressure has been dissipated and the soil is fully consolidated and drained. This means that also both the effective strength parameters (i.e. effective cohesion, c', and friction angle, ϕ') and the undrained shear strength (c_u) of sediments within the volume interested by remediation (i.e. the so-called engineering volume) are geotechnical information of paramount importance.

Therefore, the definition of an appropriate site geotechnical model is a compulsory step for the selection of potential remedy approaches. Specifically, it has to include at least the following data (USEPA 2005): (1) the soil composition and index properties; (2) the consolidation properties; (3) the strength parameters; and (4) the rates and direction of fluxes within the sediments. These data have to cover the entire engineering volume.

The aim of this study is to define a preliminary site geotechnical model, containing the essential information useful for the selection, design, placement and management of the potential mitigation solutions. The research has required an in situ investigation campaign, based on three sampling stations that have been of use also for the research groups of the National Project RITMARE for sampling the different environmental matrices (Cardellicchio et al. 2015). The geotechnical data result from an intensive investigation that has been carried out in the laboratory on both remoulded and undisturbed samples retrieved at several depths in the three stations. The research had to face with technical difficulties both in situ, for the off-shore operations that had to be carried out in a military area, and in the laboratory, for the very low consistency of the sediments from the top layer and the contaminants present, which even damaged the laboratory equipment.

The comparison of the results with others from the literature (Skempton 1970; Perret et al. 1995; Cafaro and Cotecchia 2001; Locat et al. 2002; Cotecchia et al. 2007; Levesque et al. 2007) helped in the interpretation of the site geotechnical model and shed light on some discrepancies from the expected soil mechanical response, especially with reference to the most polluted sediments within the top layer of the stratigraphic succession.

Geological setting and submarine sampling of the sediments

The geological setting of the Taranto area is characterised by the main Quaternary tectonic and sedimentary phases that involved the entire Apulian Foreland and the Bradanic Foredeep. Along the Mar Piccolo cliffs, Late Pleistocene deposits crop out with large lateral continuity (Mastronuzzi 2014; Lisco et al. 2015). In this area, the phase of extensive subsidence (Ciaranfi et al. 1988) is recorded by the thick stratum of Upper Pliocene–Lower Pleistocene Calcarenite di Gravina Formation (Azzaroli 1968; Robba 1969; Iannone

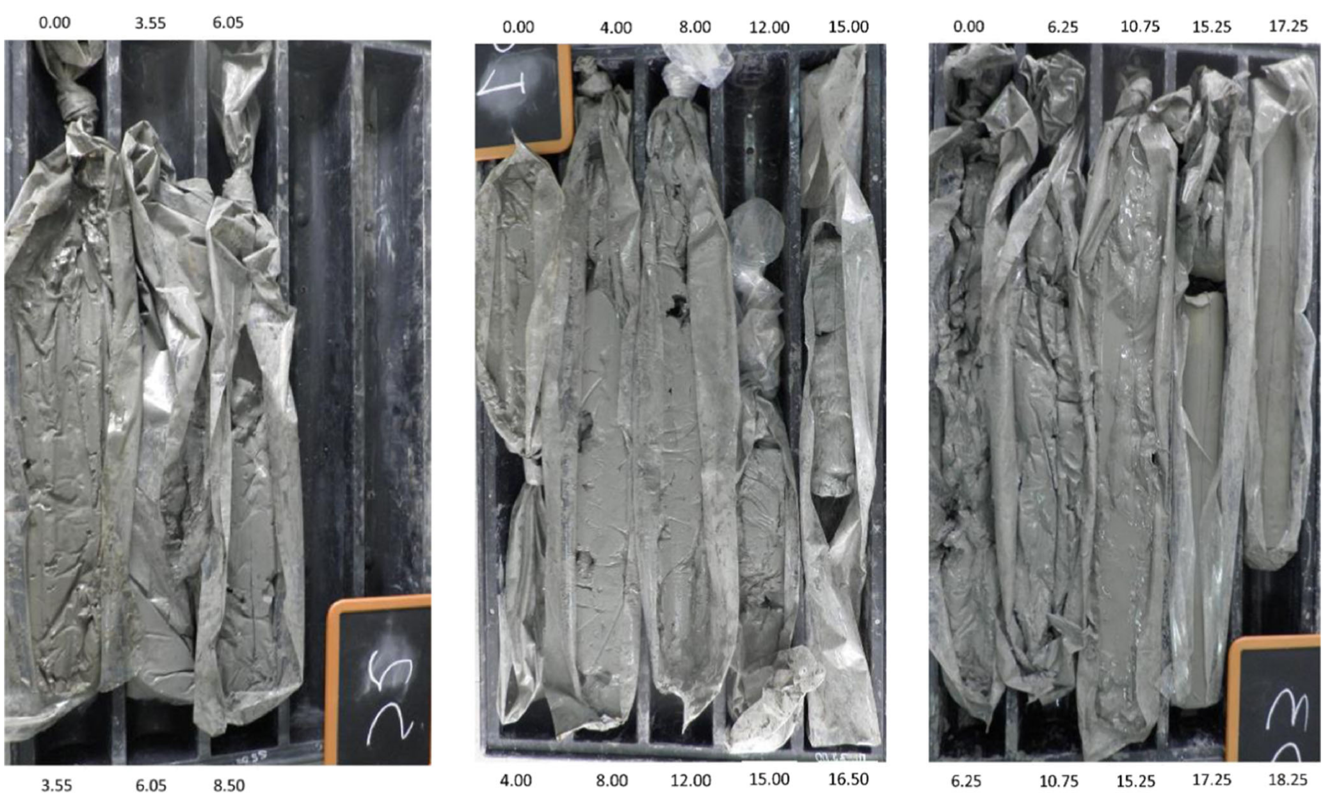

(a) (b) (c)

Fig. 2 Catalogue box of continuous corings 1I (**a**), 1L (**b**) and 1M (**c**). The length of each compartment of the catalogue boxes is 1 m. The *numbers* refer to metres of continuous coring below seafloor and Pieri 1979) which transgressively overlies Mesozoic carbonate rocks, and, in turn, is covered by the Subapennine Clays or Argille Subappennine (Azzaroli et al. 1968). They are 10 to 65 m thick and commonly known as blue clays, being grey-blue to grey-green coloured. The subsequent uplift phase, active at least from the beginning of the Middle Pleistocene (Ciaranfi et al. 1988; Ricchetti et al. 1988; Doglioni et al. 1994), is recorded by uplifted marine and fluvial terraces (Tropeano et al. 2002; Gallicchio et al. 2014; Gioia et al. 2014; Lisco et al. 2015).

The two depressions of sub-elliptical shape that constitute the Mar Piccolo are river valleys that have been incised in a continental phase (Ashley and Sheridan 1994; Zaitlin et al. 1994) and then submerged by the sea with the Holocene marine transgression (Mastronuzzi and Sansò 1998, 2002, 2003). As outlined by Cotecchia et al. (1989) and Lisco et al. (2015), the submarine stratigraphic sequence in the Mar Piccolo, from the bottom to the top, is represented by the Late Cretaceous limestone of the Calcare di Altamura Formation, the Calcarenite di Gravina Formation that passes upward in the Argille Subappennine and, finally, the Late Pleistocene–Holocene Mar Piccolo sediments. In particular, a surficial sediment thickness map has been reported by Lisco et al. (2015), resulting from sub-bottom profiler surveys (SBP Innomar 2000; frequencies, 10–12–15 kHz). According to the authors, the thickness of the shallow sediments in the first bosom ranges, on average, from 2 to 3 m. The most relevant exception is recorded in the area between the two bosoms, where a channel has been detected and the layer of recent sediments is characterised by the highest thickness, i.e. up to about 10 m (Lisco et al. 2015). The three continuous corings were carried out in proximity of this area, into the so-called 170 ha area (Fig. 1b), that is one of those prioritised for the high levels of heavy metals and organic pollutants (ICRAM-APAT 2007; ISPRA 2010). The corings were carried out by means of a drilling apparatus that was mounted on a platform previously fixed in place. Once recovered, the cores were wrapped in plastic film and placed into catalogue boxes. The quantity of material recovered was very low due to the very soft consistency of the sediments. In particular, for the shallower sediments, one catalogue box compartment (of 1 m length)

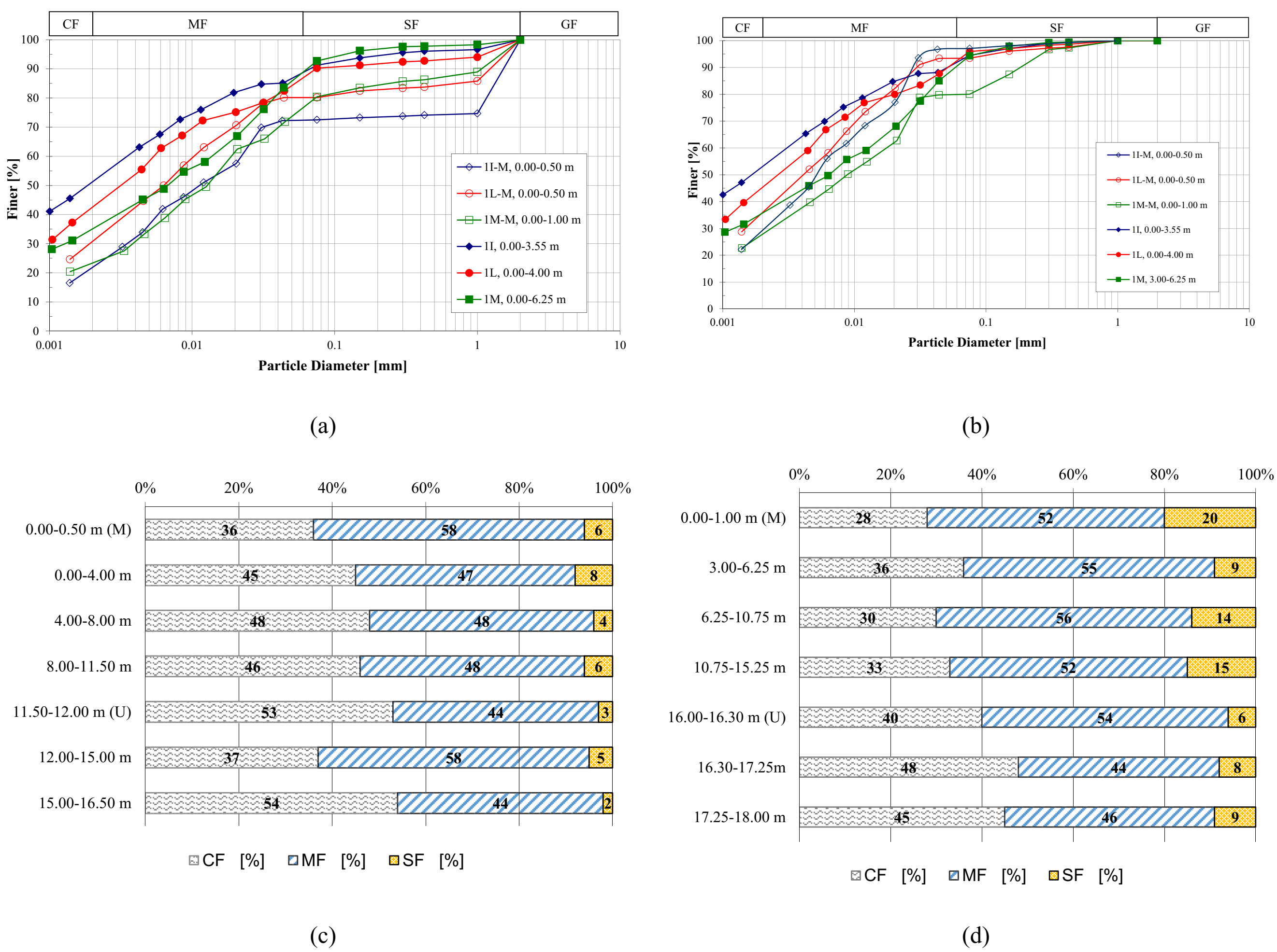

Fig. 3 **a** Grading curves within the first 6 m of sediments along the boreholes 1I, 1L and 1M. **b** The same grading curves, without particle diameters larger than 1 mm. **c** Grading fractions along borehole 1L. **d** Grading fractions along borehole 1M. Key: *CF* clay fraction, *MF* silt fraction, *SF* sand fraction, *GF* gravel fraction, *M* manual sampling, *U* undisturbed sample

could contain up to 6.5 m of sediments (Fig. 2). Samples of sediments were taken up to depths of about 20 m from the seafloor that is about the maximum depth of engineering interest in view of the placement of any mitigation solution. To the best of our knowledge, this study is the first in the Mar Piccolo that covers depths larger than 5 m below the seafloor. In particular, coring depths of 8.5, 16.5 and 18.2 m from the seafloor were reached in boreholes 1I, 1L and 1M, respectively. The sea depth in the three stations varied from 12.25 to 13.00 m. Three undisturbed samples were taken along boreholes 1L and 1M at different depths (i.e. 11.5, 16 and 18 m from the seafloor). Moreover, in proximity of the boreholes, other three samples were taken by scuba divers using 101-mm diameters PVC core samplers that were manually inserted into the first 2 m of sediments (samples 1I-M, 1L-M and 1M-M in Fig. 1b).

Geotechnical characterisation of the submarine sediments

Composition and physical properties

Figure 3a, b shows the grain-size distribution of sediment samples taken up to 6 m from the seafloor. The percentage of particles larger than 1 mm (Fig. 3a), which are mainly constituted by fragments of gastropods and bivalves, is particularly high (11–25 %) in the shallow samples taken by scuba divers (1I-M, 1L-M and 1M-M). The grading curves of the shallow samples are substantially similar, unless the highest sand fraction (*SF*) of the 1M-M sample. Samples 1I and 1L have similar silt fraction (*MF*) but higher clay fraction (*CF*) than the corresponding samples taken by scuba divers (i.e. 1I-M and 1L-M).

The vertical profiles (Fig. 3c, d) of the grading fractions at various depths below the seafloor (i.e. up to 16.50 and 18.00 m in boreholes 1L and 1M, respectively) show a trend of SF decrease and *CF* increase. Also, the sediment composition within the first 8.5 m from the seafloor of the borehole 1I confirms this trend (Table 1). Moreover, the figures show that the sediments taken from borehole 1L exhibit, in general, higher *CF* (CF_{max} = 54 %) than those sampled down borehole 1M. All these data appear to suggest a high spatial variability of the soil composition. The organic content (O) in the few samples tested is rather high (5.0 and 5.9 %) in the first metres of sediments and decreases to 0.7 % at depth (18 m below the seafloor; Table 1). The specific gravity (G_s) of the soil particles increases with depth from 2.56 to 2.74.

The plasticity properties of the sediments, determined by using distilled water (in compliance with ASTM standards), are shown in Fig. 4. The first consideration that can be made is

Table 1 Composition and physical properties of the sediments

Borehole	Depth from seafloor (m)	Composition and physical properties											
		GF (%)	SF (%)	MF (%)	CF (%)	γ (kN/m^3)	G_s (–)	w (%)	e (–)	w_L (%)	PI (%)	CI (–)	O (%)
1I/1I-M	M 0.00–0.50	0	27 (3)	51 (68)	22 (29)	13.49	2.580	170.0	4.39	85.60	49.37	−1.71	nd
	0.00–3.55	0	12 (8)	36 (39)	52 (53)	14.35	2.640	119.8	3.16	71.50	42.28	−1.14	5.0
	3.55–6.05	nd	nd	nd	nd	nd	2.714	53.1	1.44	45.79	22.78	−0.32	nd
	6.05–8.50	nd	nd	nd	nd	nd	2.734	49.5	1.35	nd	nd	nd	nd
1L/1L-M	M 0.00–0.50	0	20 (6)	49 (58)	31 (36)	13.44	2.560	163.0	4.17	86.50	47.93	−1.60	nd
	0.00–4.00	0	12 (8)	46 (47)	42 (45)	13.51	2.610	134.6	3.51	75.25	42.48	−1.40	nd
	4.00–8.00	0	4	48	48	nd	2.711	61.6	1.67	60.95	33.49	−0.02	nd
	8.00–11.50	0	6	48	46	nd	2.711	68.4	1.85	63.17	35.52	−0.14	nd
	U 11.50–12.00	0	3	44	53	17.03	2.741	51.9	1.42	60.70	37.49	0.24	nd
	12.00–15.00	0	5	58	37	nd	2.736	58.6	1.61	63.32	36.11	0.13	nd
	15.00–16.50	0	2	44	54	nd	2.736	58.5	1.60	55.25	29.41	−0.11	nd
1M/1M-M	M 00.00–1.00	0	23 (20)	54 (52)	23 (28)	13.85	2.560	170.0	4.35	79.80	40.81	−2.21	5.9
	3.00–6.25	0	12 (9)	53 (55)	35 (36)	17.22	2.650	54.2	1.43	42.25	21.03	−0.57	nd
	6.25–10.75	0	14	56	30	nd	2.719	53.9	1.47	47.47	25.28	−0.26	nd
	10.75–15.25	0	15	52	33	nd	2.714	57.4	1.56	48.57	26.32	−0.33	3.2
	U 16.00–16.30	nd	3	57	40	17.99	2.759	39.1	1.08	43.30	21.76	−0.18	nd
	16.30–17.25	0	8	44	48	nd	2.723	53.3	1.45	48.56	26.14	−0.19	nd
	17.25–18.00	0	9	46	45	nd	2.734	48.7	1.33	43.55	23.08	−0.22	0.7

Key: *M* manual sampling, *U* undisturbed sample, *GF* gravel fraction, *SF* sand fraction, *MF* silt fraction, *CF* clay fraction (percentage of fractions deprived of retained at ASTM sieve N. 18 (the particle diameters larger than 1 mm) is specified in parentheses), γ total unit weight, G_s specific gravity, w water content, e void ratio, w_L liquid limit, *PI* plasticity index, *CI* consistency index, *O* organic content, *nd* not determined

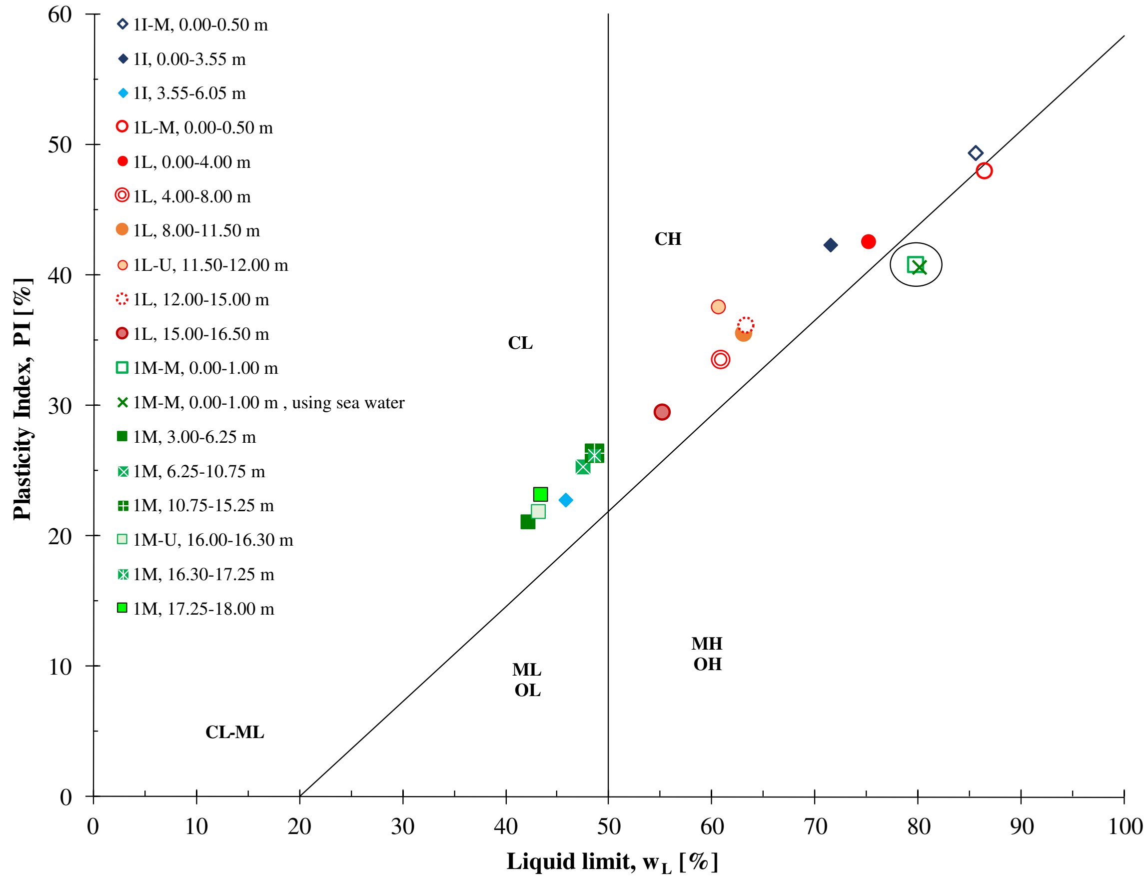

Fig. 4 Casagrande plasticity chart. In the circle, the plasticity properties of sample 1M-M are compared with those determined by using sea water

that, for all the three boreholes, both the liquid limit (w_L) and plasticity index (*PI*) tend to decrease with depth (Table 1). Despite their spatial variability, the sediments from boreholes 1L and 1I and the upper part of borehole 1M can be classified, according to the Unified Soil Classification System (USCS), as inorganic clays of high plasticity (CH) (Fig. 4), whereas those from borehole 1M, are low plasticity clays (CL). Furthermore, sample 1M-M can be classified as silt of high plasticity (MH). In Fig. 4, the plasticity properties - w_L and *PI* - of this sample are also compared with those determined by using sea water from the Mar Piccolo. The almost complete coincidence of the two determinations suggests that, at least for this sample, the plasticity properties are not appreciably affected by water salinity.

The activity (*A*) of the sediments varies between 0.5 and 1.7 (Fig. 5). In particular, the samples taken by scuba divers within the top 2 m exhibit very high activity (A_{max} = 1.3-1.7). The less active samples are those taken at larger depth.

Figure 6a, b shows that both the void ratio (*e*) and the consistency index (*CI*) of the soil samples follow similar trends when plotted against depth below sea level. The average *e* of the samples varies between 3.16 and 4.39, in the first 4 m below seafloor, to about 1.33 at depth (borehole 1M). With reference to the soil consistency, almost all *CI* values are below zero (Fig. 6b): the minimum values (about −2.2) are those of sample 1M-M and of the shallow sediments taken from 1L. It can be observed that the upper part of the stratigraphic succession, about 4 m thick, is characterised by *CI* values lower than −1.1 (Fig. 6b, c; Table 1). Below this top layer, the lower part of the stratigraphic succession exhibits a sharp decrease in void ratio, whereas the index properties do not vary significantly. This makes the soil consistency rise up to $CI = -0.55$, although remaining negative. It further increases with depth (the maximum value, $CI = 0.24$, is that of the undisturbed sample 1L-U), but values lower than zero have been recorded up to 18 m below the seafloor (borehole 1M).

In Table 2, the results of mineralogical analyses carried out on three specimens sampled down 1M borehole are reported. The X-ray diffractometry on the total sample shows the widespread presence of phyllosilicates; minor constituents are quartz, feldspars and carbonates (calcite and dolomite, while aragonite is in traces). In particular, the phyllosilicates are interstratified illite/smectite (*I/S*), chlorite/smectite (*Chl/S*), kaolinite and chlorite. Halite is also present for the marine environment from which samples have been taken and it is abundant in the shallow sample 1M-M. Moreover, hematite is significantly present, mostly dragged by the wind from the

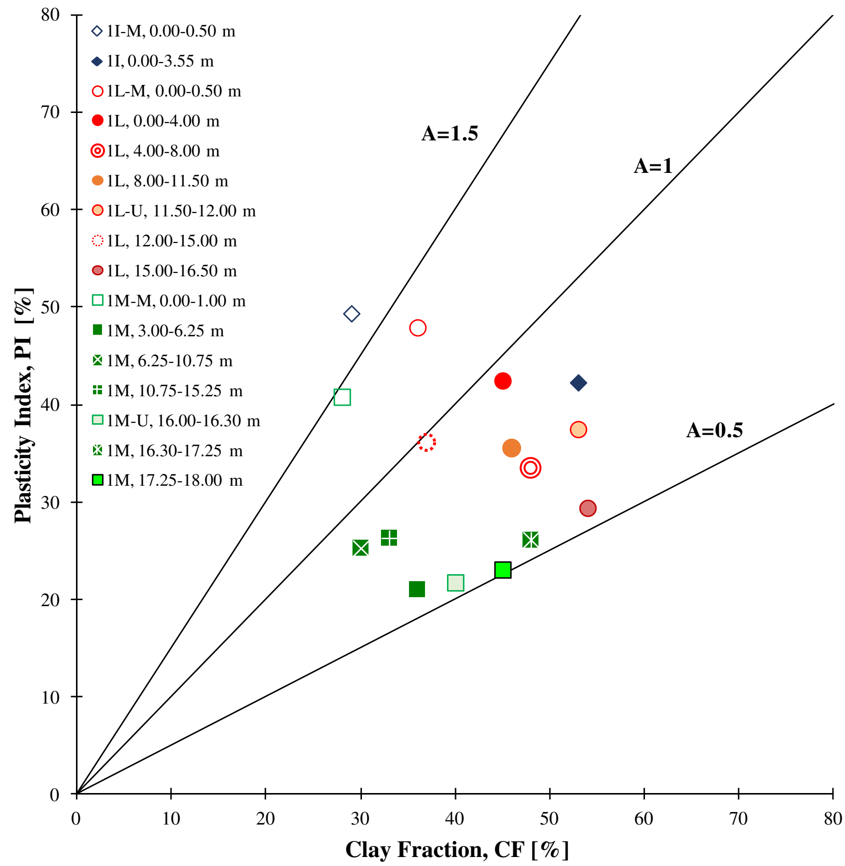

Fig. 5 Activity of the soil samples

iron ores heaps of the near steel factory. Table 2 also highlights that, except for halite and hematite, the mineralogical composition of the samples does not present significant variations with depth.

Compression and shearing behaviour of the soils

Nine oedometer tests have been carried out on samples of submarine sediments taken within the first metre up to 16.3 m below the seafloor (i.e. the specimen 1M-U). The testing programme, that has followed ASTM standards, is summarised in Table 3. The one-dimensional compression curves of the specimens are reported in Fig. 7 in the *e* - vertical effective stress (σ'_v) plane.

Samples from the top of the stratigraphic succession (i.e. the first 4 m of sediments) exhibit similar behaviour and their preconsolidation pressures (arrows in Fig. 7) seem to be either lower or equal to their overburden effective pressure (i.e. $\sigma'_p = 6–8$ kPa). As expected, the undisturbed specimens 1L-U and 1M-U, taken from 11 and 16 m below the seafloor, respectively, exhibit the higher values of preconsolidation pressures. The compression index (C_c) of the sediments (Fig. 8a) varies between about 0.7 and 1.6 in the first 4 m from the seafloor, whereas it becomes significantly lower ($C_c = 0.25–0.4$) for the three deeper specimens (i.e. 1M, 1L-U and 1M-U). The irregular trend of the compression index of the specimens taken within the first meter of sediments (Fig. 8a) has to be imputed to the presence of algae and fragments of bivalves and gastropods.

The oedometer test results are consistent with the composition and plasticity properties of the sediments: specimens 1I-M and 1L-M, of higher plasticity index (*PI*) and lower sand fraction (*SF*), exhibit higher initial void ratio and compressibility with respect to those from borehole 1M (1M-M and 1M-M2). In particular, the compression index of the top 0.5 m of sediments (specimens 1I-M and 1L-M) decreases in loading, becoming lower than 1 only for vertical effective stress values, σ'_v, higher than 100 kPa. The swelling index (C_s) varies from 0.027 (specimen 1M) to 0.092 (specimen 1L-U) (Fig. 8b).

The values of the coefficient of permeability, *k*, of the shallow to medium depth sediments are plotted in Fig. 9 against void ratio. They have been computed according to the consolidation theory by Terzaghi (1923), in both oedometer loading and unloading phases.

For all the specimens from the top 4 m of the stratigraphic succession, *k* in loading varies between $8*10^{-11}$ and $7*10^{-9}$ m/s and, in general, it decreases with void ratio. Specimens from medium depth 1M and 1L-U exhibit, for the same void

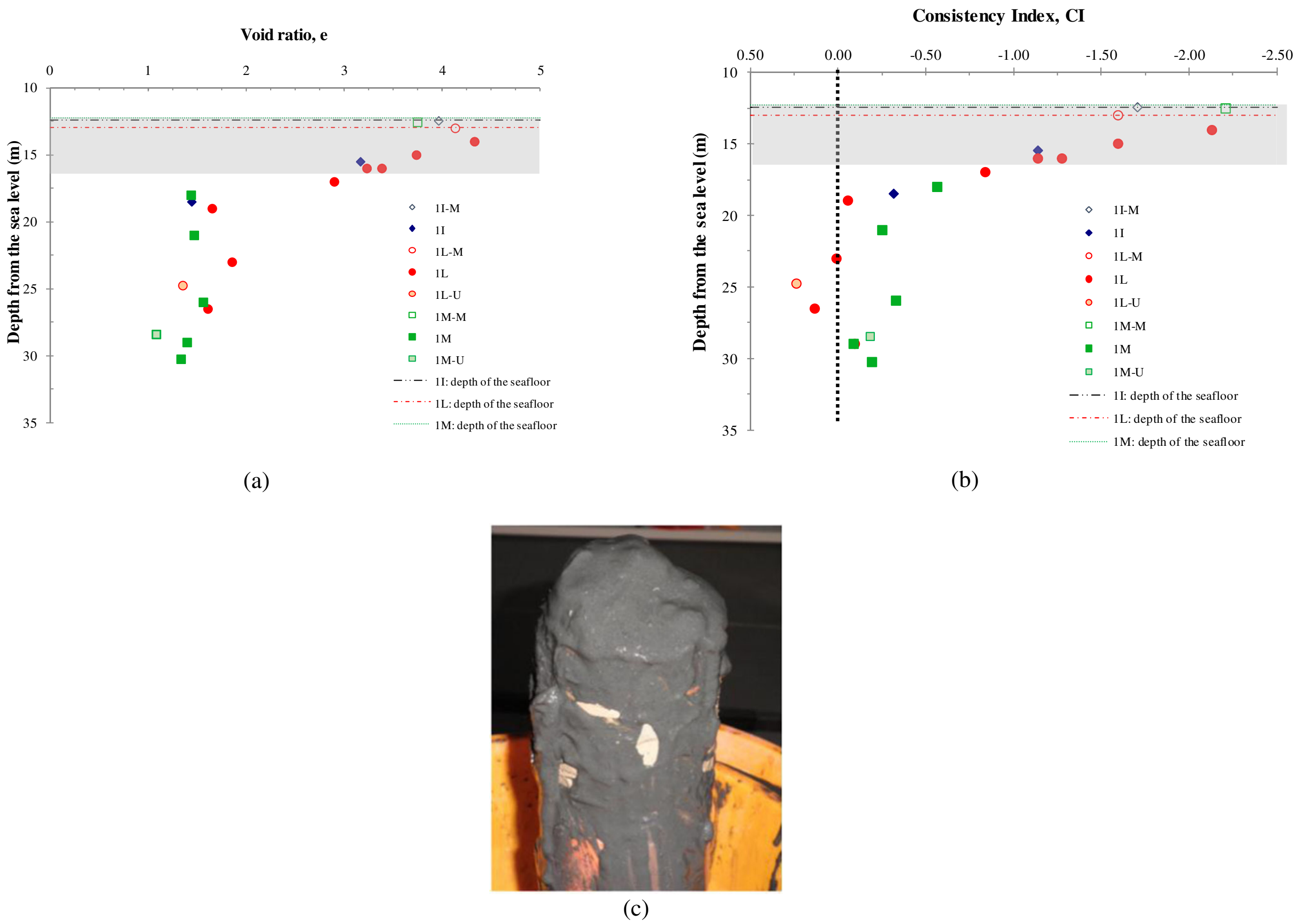

Fig. 6 Vertical profiles of **a** void ratio and **b** Consistency Index (*CI*); **c** photograph of sample 1M-M

ratios, permeability values that are higher than those of the shallower specimens of about one order of magnitude. In unloading, k is always lower than that in loading and it seems not to vary with the unloading phase ($k_{unl} = 7*10^{-12} - 2*10^{-11}$ m/s; Fig. 9).

Direct shear tests (DST) have been carried out on three specimens from sample 1I-M (0–0.5 m from seafloor). They were sheared after consolidation to vertical effective pressures from 25 to 75 kPa. In Fig. 10, the state paths followed by these three specimens during consolidation before shearing are reported together with the oedometer (OED) compression curve of the same sample. The data show that the DST specimens consolidation states lie either close or just in correspondence of the normal compression line of the OED sample. During shearing, according to their consolidation states, the specimens harden and contract up to large strains, following the so-called wet behaviour of Critical State Soil Mechanics (CSSM) (Roscoe et al. 1958; Schofield and Wroth 1968). Thus, these specimens reach a pseudo-critical state, characterised by strength parameters equal to $c' = 0$ kPa and $\varphi'_{cs} = 35°$ (Fig. 11).

The shearing behaviour of the lower part of the stratigraphic succession has been investigated by means of DST carried out on three specimens from sample 1M-U (16.0–16.3 m below the seafloor). The three specimens were consolidated from 12 to 150 kPa before shearing (Fig. 12). The oedometer

Table 2 Mineralogical composition (weight %) of the bulk sample and in the clay fraction (in parentheses)

Borehole	Depth from seafloor (m)	Qtz	K-feld	Cal	Dol	Hem	Hal	I/S + Chl/S	I	Kao	Chl
1M/1M-M	0.00–1.00	14	3	20	6	4	15	27 (60)	6 (22)	3 (11)	3 (7)
	1.00–5.00	22	6	23	7	3	4	21 (71)	8 (18)	2 (6)	2 (5)
	15.25–16.00	19	7	21	8	<1	<1	23 (62)	12 (21)	4 (10)	5 (7)

Key: *Qtz* quartz, *K-feld* feldspars, *Cal* calcite, *Dol* dolomite, *Hem* hematite, *Hal* halite, *I/S* illite/smectite, *Chl/S* chlorite/smectite, *I* illite, *Kao* kaolinite, *Chl* chlorite

Table 3 Loading sequence in oedometer tests

Borehole	Specimen	Depth from seafloor (m)	Test tipology	Loading sequence σ'_v (kPa)
1I/1I-M	1I-M	0.00–0.50	L/U	3–200–3
	1I	0.00–3.55	L	3–100
1L/1LM	1L-M	0.00–0.50	L/U	3–200–3
	1L	0.00–4.00	L	3–100
	1L-U	11.50–12.00	L/U	6–1600–25
1M/1M-M	1M-M	00.00–1.00	L/U	3–200–3
	1M-M2	00.00–1.00	L	3–100
	1M	3.00–6.25	L/U	3–200–3
	1M-U	16.00–16.30	L/U	3–6400–6

Key: *L/U* loading/unloading, *L* loading

compression curve of the same sample is also plotted (Fig. 12). As for the shallow sediments, also in this case the consolidation states before shearing of the DST specimens are consistent with those followed by the OED specimen. Moreover, according to its location in the *e*–log σ'_v plot, that is further to the left of the normal consolidation line of the 1M-U sample, the specimen sheared at lower vertical effective stress ($\sigma'_v = 12$ kPa), of overconsolidation ratio (i.e. $OCR = \sigma'_p/\sigma'_v$) equal to about 10, strain-softens (Fig. 13a) and dilates (Fig. 13b) according to the so-called *dry behaviour* of CSSM. On the contrary, the specimen sheared at $\sigma'_v = 150$ kPa exhibits a *wet behaviour* according to the OCR value, that is equal to 1 (Fig. 13a, b). The third specimen, that has been sheared at 50 kPa, has an intermediate behaviour, i.e. still in agreement with its OCR value (OCR = 2). The soil strength parameters at peak are $c'_p = 15$ kPa and $\phi'_p = 23.1°$, whereas the friction angle at critical state is about $\phi'_{cs} = 27.8°$ (Fig. 14).

Discussion of the results

The results show that, despite their spatial variability, the sediments in the investigated area appear to be normally consolidated silty clays (or clayey silts) up to medium depths below seafloor. This means that they have never been under effective pressures greater than those existing at the present time.

Figure 4 shows that the soil samples lie within a narrow band above the A-line in the plasticity chart (Casagrande 1948), that is a relationship typical of sedimentary clays having low carbonate and organic material content. This is also confirmed by the organic content (Table 1) that is higher than 5 % only for one sample (1M-M; $O = 5.9$ %), whose point is located slightly below the A-line in Fig. 4.

For the investigated sediments, a rate of deposition (*r*) of about 1 mm/year, which is typical of Holocene clays (Skempton 1970), has been estimated (Mastronuzzi 2014).

Fig. 7 Loading/unloading oedometer compression curves of the samples

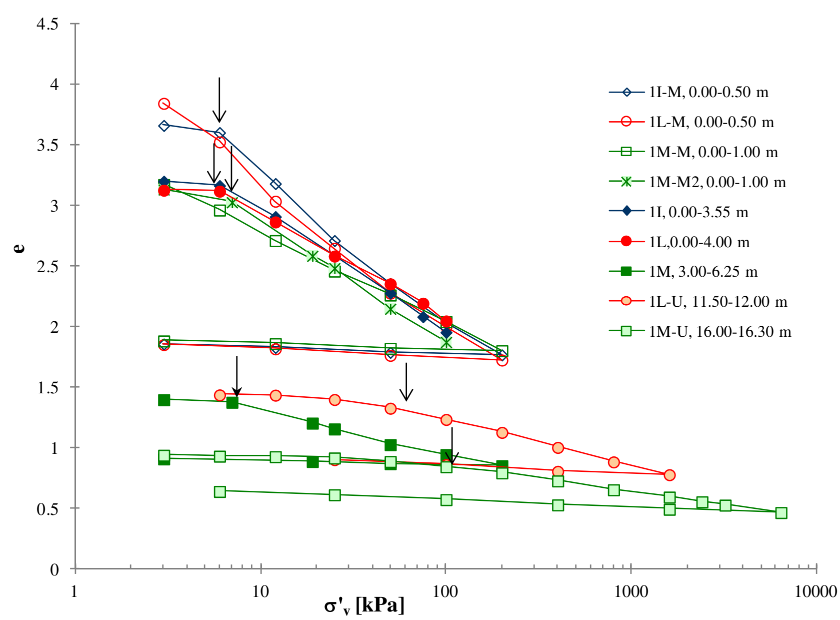

Fig. 8 **a** Compression index versus vertical effective stress; **b** swelling index versus vertical effective stress

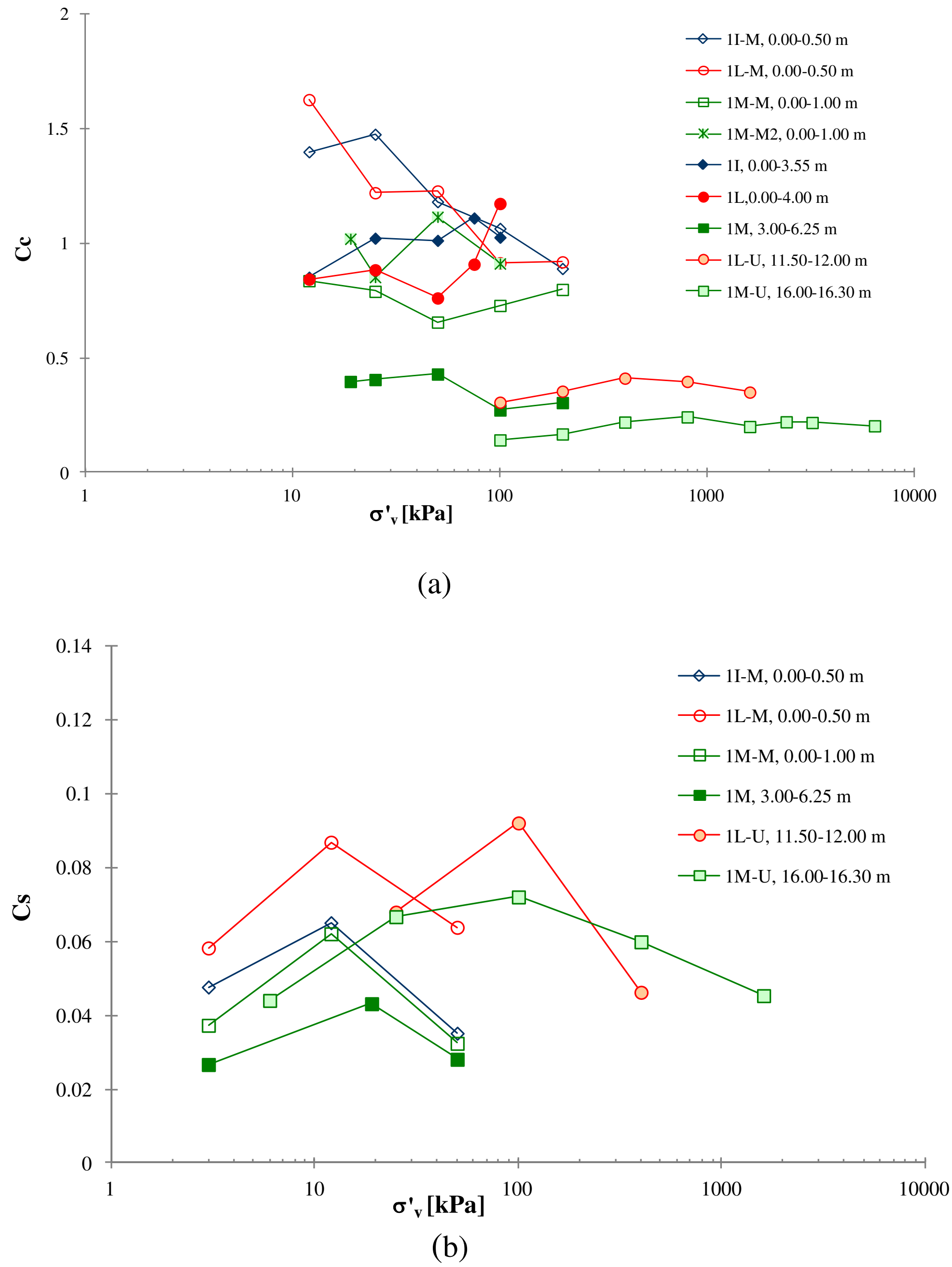

Although theoretically a clay can be fully consolidated with infinitely slow deposition, experiments suggest that 95 % consolidation can be assumed as a sufficiently close approximation to final equilibrium. Gibson (1958) showed that for this degree of consolidation to be reached in a clay, with a uniform rate of deposition, the ratio c_v/rh must be lower than 10; where h is the thickness of the layer and c_v is the consolidation coefficient of the clay. For $r=1$ mm/year and $c_v=1$ m^2/year, the sediments are more than 95 % consolidated provided their thickness is less than 100 m, which is a condition widely satisfied by the present study.

Under this experimental conditions, Skempton (1970) has shown that, at any particular overburden pressure, the water content of a normally consolidated clay has to be directly related to the Atterberg limits, that reflect both the nature and amount of clay minerals. Therefore, if the water content, the effective overburden pressure and the Atterberg limits are known for an individual layer of normally consolidated clay, it is possible to reconstruct the entire sedimentation compression curve (SCC) for that clay. In the following, the consistency of some of these relevant geotechnical correlations for normally consolidated deposits is checked for the soils here of reference.

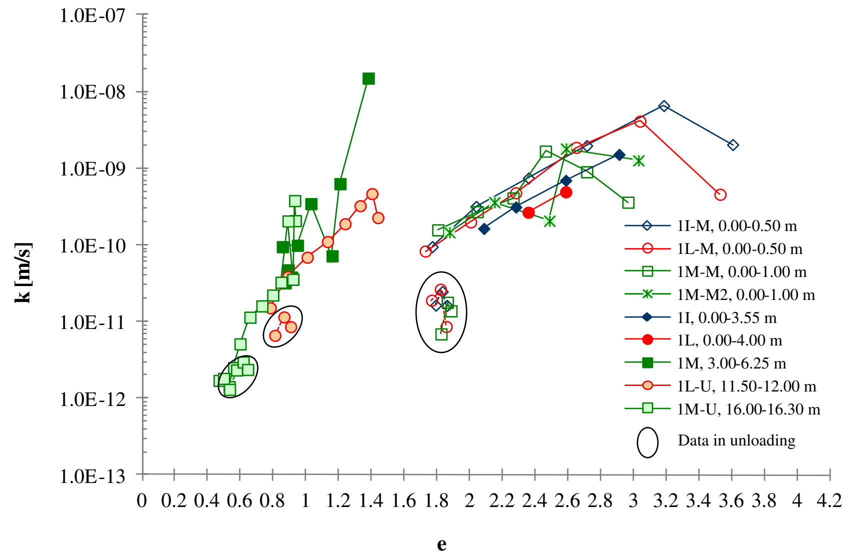

Fig. 9 Coefficient of permeability versus void ratio (data in loading and unloading)

The recent sediments from the top of the stratigraphic succession

In Fig. 15 the sedimentation compression curves presented by Skempton (1970) for 20 normally consolidated clayey deposits are shown. Several of these data are from clayey sediments recently deposited on the seafloor and taken within the top 10 m. They often have clay fraction and Atterberg limits (e.g. Oslofjord, A-31 and Gosport samples in Fig. 15) similar to those of the sediments sampled from the Mar Piccolo. By analysing the void ratio-effective overburden pressure data relative to the samples taken from the first bosom of Mar Piccolo (Fig. 15), it can be concluded that only the data relative to the sediments taken below the top layer (about 4 m thick) lie about the SCC corresponding to their w_L (see Table 1). On the contrary, the consolidation states of the sediments from the top of the stratigraphic succession lie on other SCCs that correspond to w_L values that are between 100 and 115 % (i.e. higher than those determined). For a fixed range of effective overburden pressures, this can be due either to higher void ratios or to lower liquid limits of the sediments with respect to those expected according to the literature data. These results also explain the very low *CI* values that are measured especially in the top layer and that are not justified by higher consistency that is instead exhibited by the shallow sediments (see Fig. 6c). In particular, according to geotechnical standards, the measured *CI* should physically correspond to a totally liquid consistency not only in the top layer but also up to about 11 m below the seafloor.

In Fig. 16, the oedometer compression curves shown in Fig. 7 are re-plotted in terms of liquidity index, *LI* (=1 − *CI*), versus vertical effective stress, σ'_v. In the same figure, the narrow band identified by Skempton (1970) by plotting the same data of Fig. 15 is reported. It can be observed that only the data of the Mar Piccolo sediments below the top layer are included into this narrow band. Moreover, in the same figure

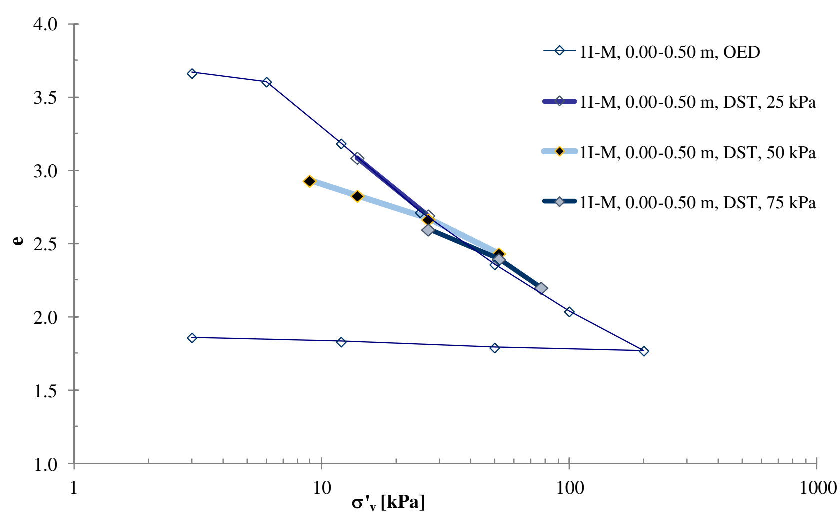

Fig. 10 Sediments from the top layer: consolidation states during compression in oedometer (*OED*) and direct shear tests (*DST*)

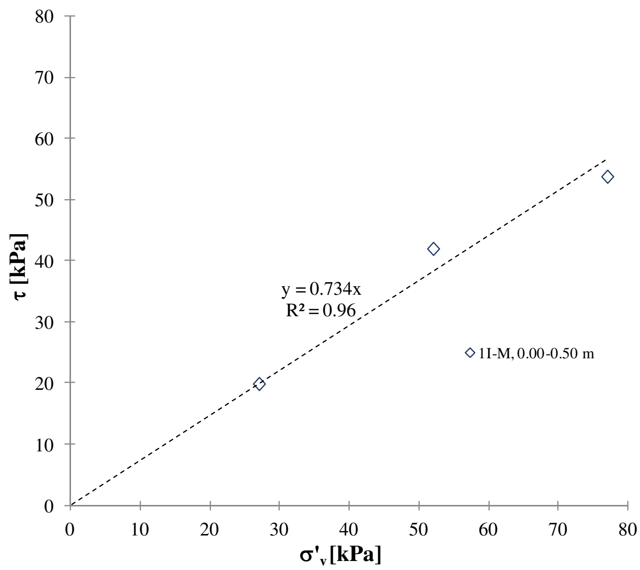

Fig. 11 Sample 1I-M, 0.00–0.50 m depth below seafloor: direct shear test results

three compression curves followed by samples of recent submarine (not polluted) hemipelagic sediments taken within 12 m below the seafloor from the Saguenay Fjord are also reported (Perret 1995; Perret et al. 1995; Martin et al. 2001; Locat et al. 2002; Levesque et al. 2007). In terms of composition, organic content and physical properties, these normally consolidated soils are similar to those found in the top layer of the first bosom of Mar Piccolo. However, despite these similarities, it can be observed that, differently from the soils under study, they lie within the band identified by Skempton for normally consolidated argillaceous deposits. These data seem to confirm that the top layer is characterised by either much higher water contents or much lower liquid limits than they would have been under normal consolidation conditions.

Similar results have been found by Levesque et al. (2007) in the North Arm and Ha!Ha Bay in the Saguenay Fjord (Canada) in a succession of submarine sediments that have been heavily polluted due to the industrial activity in the area (Pelletier et al. 2003). The authors hypothesised that such experimental discrepancy could be due to bioturbation. In this respect, it has to be noticed that there is no significant bioturbation in the area under study (Tursi and Mastrototaro 2013), but this part of the stratigraphic succession is the most polluted since it contains the highest concentrations of organic pollutants and heavy metal cations (ICRAM-APAT 2007).

These results suggest that the changes in pore fluid chemical composition and viscosity (due to the high content of contaminants in situ) are leading both ion exchange and variations in the mechanical properties of the sediments in the upper part of the stratigraphic succession. This conclusion is supported by several laboratory test results on chemo-mechanical interactions in kaolinite, smectite and mixed clay samples prepared with solutions of different chemical compositions (e.g. Meegoda and Ratnaweera 1994; Chen et al. 2000; Calvello et al. 2005; Gajo and Maines 2007; Wahid et al. 2011a, b to cite the most recent ones). Moreover, Santamarina et al. (2001) underline that the potential of chemical–mechanical coupling is greatest in fine-grained soils at low confinement (i.e. the conditions of the sediments here of reference) and that such coupling may lead to unforeseen results because of the complexity of the clay fabric formation and the interaction between multiple internal scales.

From what above, it comes out the need of separate investigations aiming to deepen the effect of contaminants on the geotechnical properties of the sediments from the top layer.

The clayey soils from the lower part of the stratigraphic succession

The composition and plasticity properties of the soils below the top layer are similar to those of the clay samples taken from the locations B and P in Fig. 17 in the Montemesola

Fig. 12 Sample 1M-U, 16.00–16.30 m depth below seafloor: consolidation states during compression in oedometer (*OED*) and direct shear tests (*DST*)

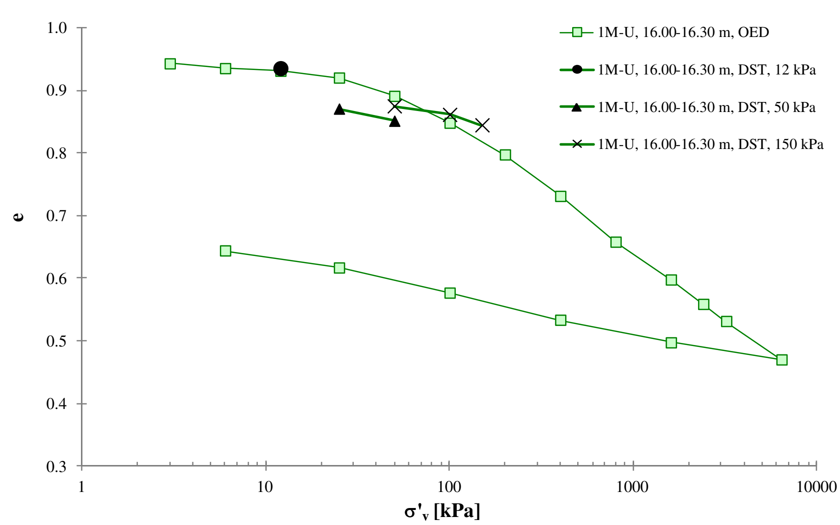

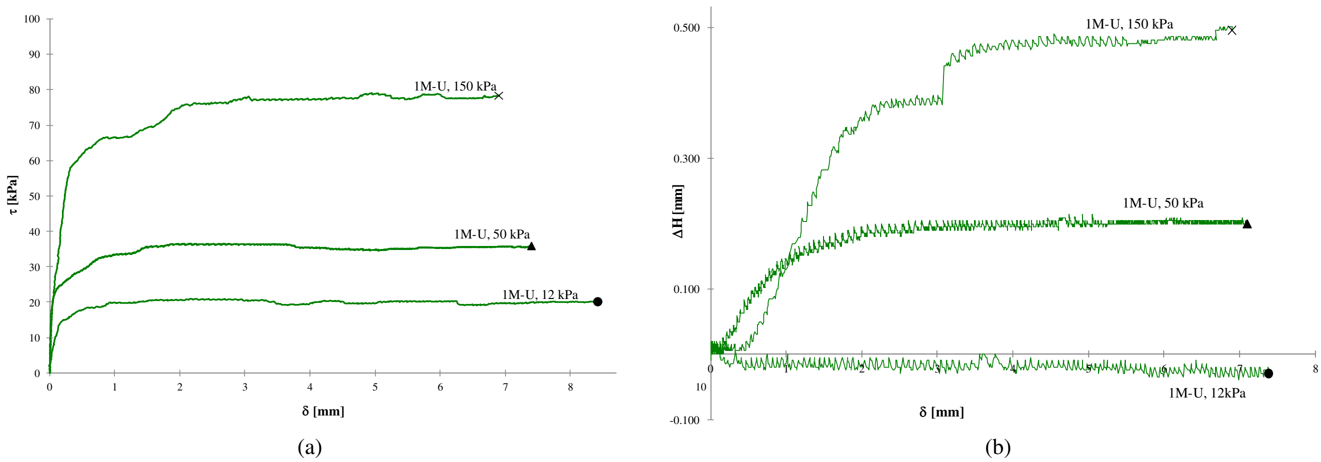

Fig. 13 Direct shear test results (sample 1M-U, 16.00–16.30 m depth below seafloor): **a** shear stress versus horizontal displacement; **b** vertical settlement versus horizontal displacement

Basin (Table 4), near the Mar Piccolo (De Marco et al. 1981; Cotecchia and Chandler 1997; Cafaro and Cotecchia 2001; Cotecchia et al. 2007). These samples belong to the stiff clay deposit of Argille Subappennine present in the Montemesola Basin.

The comparison between the clay samples retrieved by the different sites in the Basin shows that their variability in composition and plasticity is similar to that recorded between the samples of this study. Their variability has to be linked to the different deposition conditions: clay sedimentation occurred in a quiet sea at site P, whereas more turbulent deposition conditions have characterised the edges of the Basin (site B). Moreover, also the mineralogy of the clays from the Montemesola Basin, that is mainly illitic with significant presence of both smectite and kaolinite (Garavelli and Nuovo 1974; Cotecchia and Chandler 1995, 1997), is quite similar to that of the Mar Piccolo sediments. However, it has to be noted that, differently from the Mar Piccolo sediments, the unloading due to erosion is the main cause of overconsolidation in the whole basin, so that the clays from Montemesola are overconsolidated clays and their consistency is higher than that of the sediments (CI = 1.01–1.05; Table 4).

In Fig. 18, the compression curves of samples 1M-U and 1M are compared with the data reported by Cotecchia et al. (2007) for two reconstituted samples (P19* and Bg*) of similar composition (Table 4). Following Burland (1990), the compression curves of the reconstituted samples represent the intrinsic compression lines (ICLs) of the clays. The figure shows that the behaviour of samples 1M-U and 1M is similar to that of samples P19* and Bg*. This would confirm that the soils from the lower part of the stratigraphic

Fig. 14 Sample 1M-U, 16.00–16.30 m depth below seafloor: strength parameters from direct shear tests

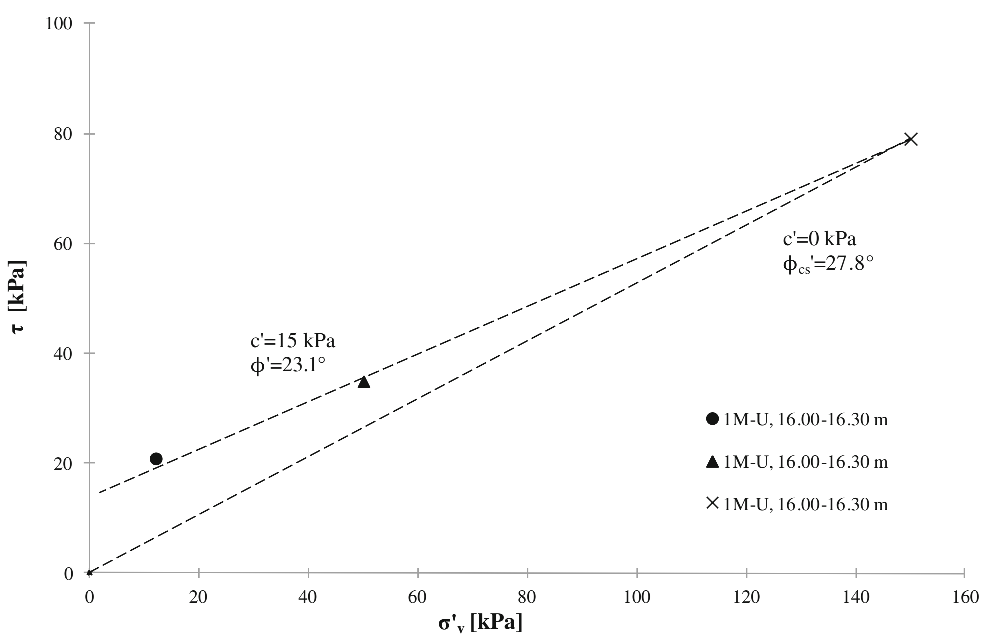

Site	w_L [%]	Site	w_L [%]	Site	w_L [%]
St. Andrew Bay	108	Tilbury	112		
Oslofjord	98	Älvängen	95		
A-33	80	G. d. Messico	87	S. Joaquin	64
A-31	63	Gosport	80	Milazzo	62
B-87	58	Pisa	72	Kambara	-
		Avonmouth	71		
		Drammen	57		
C-18	46	Grangemouth	41	Baku	40
		Drammen	38	Valle del Po	-
		Detroit	25		

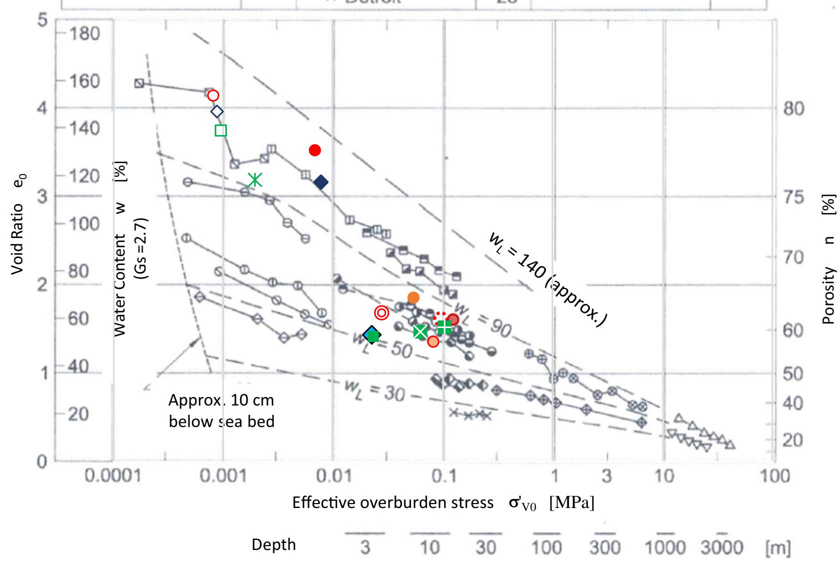

Borehole	w_L [%]	Borehole	w_L [%]	Borehole	w_L[%]
1I-M, 0.00-0.50 m	85.60	1I, 0.00-3.55 m	71.50	1I, 3.55-6.05 m	45.79
1L-M, 0.00-0.50 m	86.50	1L, 0.00-4.00 m	75.25	1L, 4.00-8.00 m	60.95
1L, 8.00-11.50 m	63.17	1L-U, 11.50-12.00 m	60.70	1L, 12.00-15.00 m	63.32
1L, 15.00-16.50 m	55.25	1M-M, 0.00-1.00	79.80	1M-M2, 0.00-1.00 m	79.80
1M, 3.00-6.25 m	42.25	1M, 6.25-10.75 m	47.47	1M, 10.75-15.25 m	48.57

Fig. 15 Sedimentation compression curves for normally consolidated clayey sediments (after Skempton 1970, modified). Data in the table at the top of the figure are from Skempton (1970); data in the table at the bottom of the figure are from this study

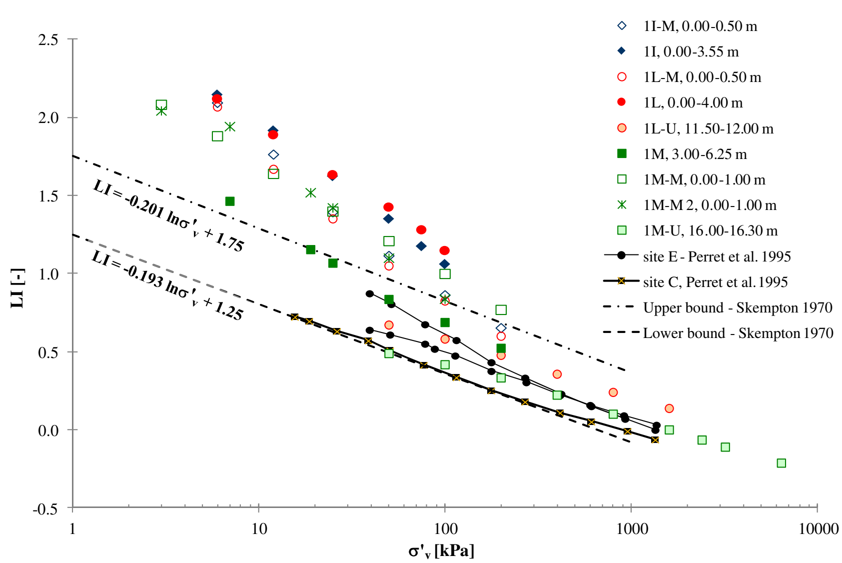

Fig. 16 Liquidity index versus vertical effective pressure (data from this study, from Perret et al. 1995; Skempton 1970)

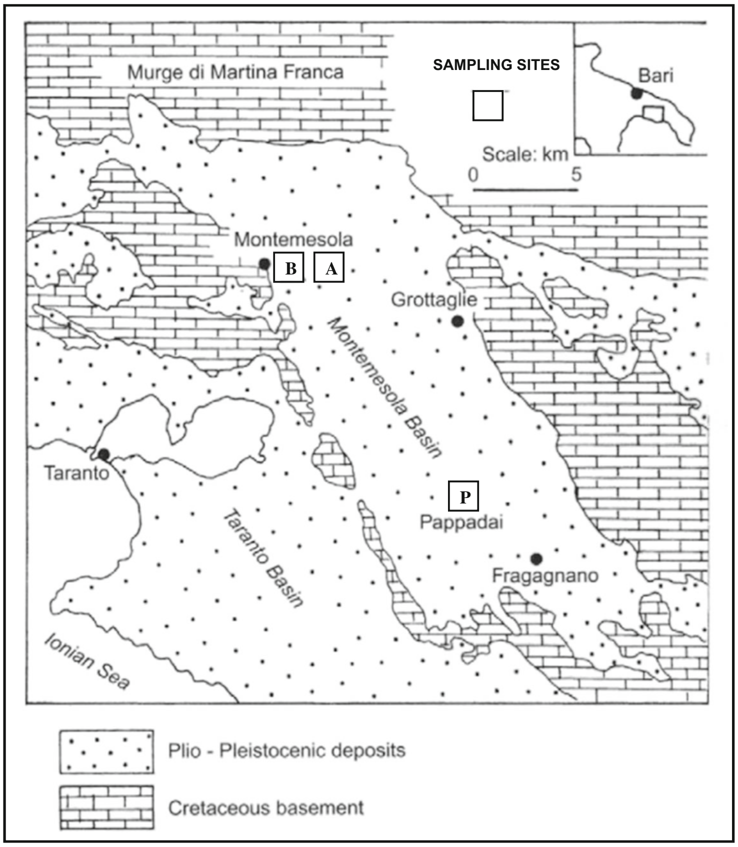

Fig. 17 Montemesola Basin and sampling sites

succession (i.e. below the top polluted layer) can be attributed to the Argille Subappennine. However, their compression behaviour is similar to that of the reconstituted clay since the compression curves of samples 1M-U and 1M almost coincide with the ICLs of samples P19* and Bg*.

Preliminary geotechnical model of the investigated area

Figure 19 reports the preliminary geotechnical model of the investigated area, containing average information about the sediment composition, physical properties, permeability, compression and shearing behaviour. The model reports to the sedimentary units by Cotecchia et al. (1989) and Lisco et al. (2015) where, from the top to the bottom, up to depths of engineering interest, the stratigraphy of the investigated area is characterised by the unit of the Mar Piccolo sediments (e1; Late Pleistocene - Holocene) and the unit of the so-called Argille Subappennine (ASP; Late Pliocene–Early Pleistocene). As shown in Fig. 19, from a geotechnical point of view, the sedimentary unit e1 has to be divided into two geotechnical units: e1-a and e1-b. The first one is likely representing an *artificially modified geotechnical unit*, whose physical and mechanical properties do not seem to be those expected according to the soil natural history. On the contrary, they can be explained only as the effect of the chemo-mechanical coupling induced in the natural sediments by pore fluids of altered viscosity and chemical composition. Moreover, it has to be underlined that the model is representing average

Table 4 Index and physical properties of the clays sampled at the two sites of the Montemesola basin (data from Cotecchia et al. 2007)

Site	Sample	Depth (m below g.l.)	CF (%)	G_s (–)	w (%)	e (–)	w_L (%)	PI (%)	CI (–)
Site B	BG	Base of quarry wall	49	2.71	23.6	0.65	51.1	27.7	1.05
Site P	P19	19	52	2.74	22.7	0.63	51.8	28.8	1.01

Key: *CF* clay fraction, G_s specific gravity, w water content, e void ratio, w_L liquid limit, *PI* plasticity index, *CI* consistency index

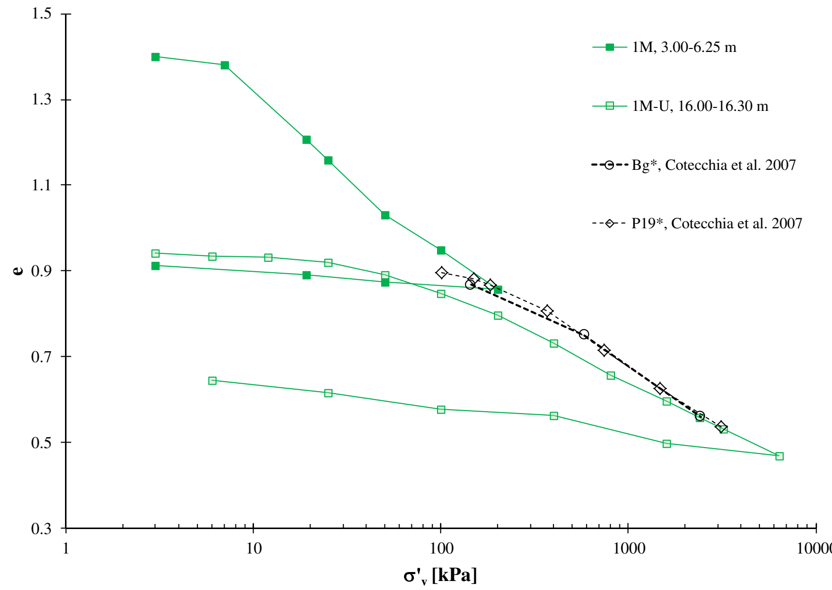

Fig. 18 Compression behaviour of the sediments below the top layer from the Mar Piccolo and of the Argille Subappennine from the Montemesola Basin (data from this study and from Cotecchia et al. 2007)

values of the geotechnical data, not accounting for the heterogeneity that has been recognised between the borehole vertical 1M and the other two, 1I and 1L. The data reported in the model for the ASP unit are those taken from the deepest sample (1M; 17.2–18.0 m below seafloor).

With respect to the in situ hydrogeological conditions, it should be noted that the mineralogical analyses have shown halite contents decreasing with depth (Table 2). This result confirms the vertical ascending flow of fresh ground water coming from the Mesozoic carbonate artesian aquifer below.

Conclusions and perspectives

The geotechnical characterisation of the submarine sediments located in the most polluted area within the first bosom of Mar Piccolo in Taranto has been carried out by means of site investigations and laboratory testing, which resulted to be complex given the off-shore sampling, the sediment very soft consistency and the high percentages of contaminants.

An original result of the research is the preliminary geotechnical model of the area investigated (Fig. 19). It covers the

Sedimentary units[(1)]	Geotechnical units	Thickness	CF	SF	G_S	e_0	PI	CI	O	Cc	Cs	k_{load}	ϕ'_{cs}
		[m]	[%]	[%]	[-]	[-]	[%]	[-]	[%]	[-]	[-]	[m/s]	[°]
e1	e1-a 	0 to 2-4m below the seafloor	38	18	2.56-2.65	3.16-4.39	45	-2.2--1.1	5-6	0.7-1.6	0.03-0.09	$8*10^{-11}$-$7*10^{-9}$ (Δe =2.0-3.0)	35
	e1-b 	2-4 to about 16m below the seafloor	44	8	2.71-2.74	1.45-1.85	30	-0.6-+0.1	3	0.4	0.03-0.09	$2*10^{-12}$-$2*10^{-10}$ (Δe =0.4-1.4)	28
ASP	ASP 	from about 16m below the seafloor	nd	nd	2.74	1.33	23	-0.2	0.7	nd	nd	nd	nd

Fig. 19 Preliminary geotechnical model of the investigated area. (1) Sedimentary units reported in the geological model by Lisco et al. (2015). Key: *CF* average values of clay fraction, *SF* average values of sand fraction, G_s specific gravity, e_0 void ratio, *PI* average values of plasticity index, *CI* consistency index, *O* organic content, *Cc* compression index, *Cs* swelling index, k_{load} coefficient of permeability in loading (the range of the corresponding void ratio is specified in parentheses), ϕ'_{cs} friction angle at pseudo-critical state, *nd* not determined

engineering volume and contains information about soil composition, physical properties, permeability, compression and shearing behaviour, which are relevant for the design of mitigation or reclaim strategies.

The key conclusions from this study relating to the site geotechnical characterisation are as follows: (1) despite the data spatial variability, the soils can be classified as normally consolidated either silty clays or clayey silts and their highest organic content is about 6 %; (2) up to 18 m below the seafloor, the vertical profile of the consistency index is characterised by values almost always lower than zero; (3) a 4-m thick top layer has been identified, where the polluted sediments have lower consistency index, higher void ratio and compressibility (C_c is almost always higher than 1) than the soils from higher depths; (4) the shearing behaviour of the sediments seems to be consistent with Critical State Soil Mechanics; and (5) the comparison with other data from the literature has allowed us to demonstrate that the soils below the top layer are part of the Argille Subappennine, although their behaviour seems to be that of the reconstituted clay.

The soils here of reference belong to that class of normally consolidated materials, whose void ratio, at a given effective overburden pressure, should depend on the liquid limit, given that it reflects the nature and the amount of clay minerals present. However, this study puts in evidence that only the sediments below the top layer (i.e. unit e1-b in the geotechnical model in Fig. 19), that are less polluted, follow the standard correlations. On the contrary, the volumetric response of the most polluted layer of sediments (i.e. the geotechnical top unit e1-a in Fig. 19) due to gravitational compaction, is characterised by discrepant behaviour. These sediments are likely representing an *artificially modified geotechnical unit*, whose physical and mechanical properties do not seem to be those expected according to the soil natural history. On the contrary, they can be explained only as the effect of the chemo-mechanical coupling induced in the natural sediments by pore fluids of altered viscosity and chemical composition. Further studies should deepen this aspect of the research by focusing on the effect of pollutants on the soil geotechnical characterisation.

Acknowledgements The activities described in this publication were funded by the Agency for Environmental Protection of the Apulia Region (ARPA-Puglia) in the South of Italy. The authors are grateful to the technician Angelo Miccoli for his help in experimental laboratory testing.

References

Ashley GM, Sheridan RE (1994) Depositional model for valley fills on a passive continental margin. In: Dalrymple RW, Boyd RJ, Zaitlin BA (eds) Incised-valley systems: origin and sedimentary sequences. SEPM Spec Publ 51:285–301

Azzaroli A (1968) Calcarenite di Gravina. Studi illustrativi della Carta Geologica d'Italia-Formazioni geologiche. Servizio Geologico d'Italia 1:183–185

Azzaroli A, Perno U, Radina B (1968) Note illustrative della Carta Geologica d'Italia. Foglio 188 – Gravina di Puglia. Servizio Geologico d'Italia pp. 57

Burland JB (1990) On the compressibility and the shear strength of natural clays. Geotechnique 40(3):329–378

Cafaro F, Cotecchia F (2001) Structure degradation and changes in the mechanical behaviour of a stiff clay due to weathering. Geotechnique 51(5):441–453

Calvello M, Lasco M, Vassallo R, Di Maio C (2005) Compressibility and residual shear strength of smectitic clays: influence of pore aqueous solutions and organic solvents. Rivista Italiana di Geotecnica 1:34–47

Cardellicchio N, Buccolieri A, Giandomenico S, Lopez L, Pizzulli F, Spada L (2007) Organic pollutants (PAHs, PCBs) in sediments from the Mar Piccolo in Taranto (Ionian Sea, Southern Italy). Mar Pollut Bull 55:451–458

Cardellicchio N, Buccolieri A, Di Leo A, Librando V, Minniti Z, Spada L (2009) Methodological approach for metal pollution evaluation in sediments collected from the Taranto Gulf. Toxicol Environ Chem 91(7):1273–1290

Cardellicchio N, Annicchiarico C, Di Leo A, Giandomenico S, Spada L (2015) The Mar Piccolo of Taranto: an interesting marine ecosystem for the environmental problems studies. Environ Sci Pollut Res. doi: 10.1007/s11356-015-4924-6

Casagrande A (1948) Classification and identification of soils. Trans Am Soc Civ Eng 113:901–930

Chen J, Anandarajah A, Inyang H (2000) Pore fluid properties and compressibility of kaolinite. J Geotech Geoenviron 126(9):798–807

Ciaranfi N, Pieri P, Ricchetti G (1988) Note alla carta geologica delle Murge e del Salento (Puglia centro-meridionale). Mem Soc Geol Ital 41:449–460

Cotecchia F, Chandler RJ (1995) The geotechnical properties of the Pleistocene clays of the Pappadai valley, Taranto, Italy. Quart J Eng Geol 28:5–22

Cotecchia F, Chandler RJ (1997) The influence of structure on the pre-failure behaviour of a natural clay. Geotechnique 47(3): 523–544

Cotecchia F, Cafaro F, Aresta B (2007) Structure and mechanical response of sub-Apennine blue clays in relation to their geological and recent loading history. Geotechnique 57(2):167–180

Cotecchia V, Lollino G, Pagliarulo R, Stefanon A, Tadolini T, Trizzino R (1989) Studi e controlli in situ per la captazione della sorgente sottomarina Galeso, Mar Piccolo di Taranto. Proceedings of the Int. Congress of Geo-engineering, Associazione Mineraria Subalpina, Torino, 1:475–484

De Marco A, Moresi M, Nuovo G (1981) Le argille dei bacini di Taranto e di Grottaglie-Montemesola: caratteri granulometrici, mineralogici e chimici. Rend Soc It Min Petr 37(1):241–266

Di Leo A, Annicchiarico C, Cardellicchio N, Spada L, Giandomenico S (2013) Trace metal distributions in Posidonia oceanica and sediments from Taranto Gulf (Ionian Sea, Southern Italy). Mediter Marine Sci 14(1):204–213

Doglioni C, Mongelli F, Pieri P (1994) The Puglia uplift (SE Italy): an anomaly in the foreland of the Apenninic subduction due to the buckling of a thick lithosphere. Tectonics 13(5):1309–1321

Eek E, Godøy O, Aagaard P, Breedveld GD (2007) Experimental determination of efficiency of capping materials during consolidation of metal-contaminated dredged material. Chemosphere 69:719–728

Federico A, Vitone C (2014) Caratterizzazione geotecnica dei sedimenti superficiali del I seno del Mar Piccolo di Taranto. Technical report for the Italian Environmental Protection Agency

Gajo A, Maines M (2007) Mechanical effects of aqueous solutions of inorganic acids and bases on a natural active clay. Geotechnique 57(8):687–699
Gallicchio S, Moretti M, Spalluto L, Angelini S (2014) Geology of the middle and upper Pleistocene marine and continental terraces of the northern Tavoliere di Puglia plain (Apulia, southern Italy). J Maps 10(4):569–575
Garavelli CL, Nuovo G (1974) Le argille di Montemesola: dati mineralogici e chimici. Rend Soc It Miner Petr 30:611–642
Gibson RE (1958) The progress of consolidation in a clay layer increasing in thickness with time. Geotechnique 8:171–182
Gioia D, Gallicchio S, Moretti M, Schiattarella M (2014) Landscape response to tectonic and climatic forcing in the foredeep of the southern Apennines, Italy: insights from quaternary stratigraphy, quantitative geomorphic analysis, and denudation rate proxies. Earth Surf Process Landf 39(6):814–835
Iannone A, Pieri P (1979) Considerazioni critiche sui "Tufi calcarei" delle Murge Nuovi dati litostratigrafici e paleoambientali. Geografia Fisica e Dinamica Quaternaria 2:173–186
ICRAM-APAT (2007) Manuale per la movimentazione di sedimenti marini. Technical report. http://www.isprambiente.gov.it/contentfiles/00006700/6770-manuale-apat-icram-2007.pdf
ISPRA (2010) Elaborazione e valutazione dei risultati della caratterizzazione ai fini della individuazione degli opportuni interventi di messa in sicurezza e bonifica del sito di interesse nazionale di Taranto. Technical report. http://www.va.minambiente.it/it-IT/Oggetti/MetadatoDocumento/76634
Italian Law n. 349 (1986) Istituzione del Ministero dell'Ambiente e norme in materia di danno ambientale. Gazzetta Ufficiale della Repubblica Italiana n. 162 del 1986
Italian Law n. 426 (1998) Nuovi interventi in campo ambientale. Gazzetta Ufficiale della Repubblica Italiana n. 291 del 1998
Italian Law n. 129 (2012) Disposizioni urgenti per il risanamento ambientale e la riqualificazione del territorio della città di Taranto. Gazzetta Ufficiale della Repubblica Italiana n. 184 del 2012
Lee LT (2001) In situ expedient test methods to determine geotechnical properties of dredged materials. DOER Technical notes collection (ERDC TN- DOER –N12), US Army Engineer Research and Development Center, Vicksburg, MS. www.wes.army.mil/el/dots/doer
Lenhart JJ, Lee J, Hwang Y, Fox PJ (2009) Polychlorinated biphenyl transport from consolidation of contaminated sediments during in situ capping. ASTM JAI 6(8):68–85. doi:10.1520/JAI102160
Lerario VL, Giandomenico S, Lopez L, Cardellicchio N (2003) Sources and distribution of polycyclic aromatic hydrocarbons (PAHs) in sediments from the Mar Piccolo of Taranto, Ionian Sea, Southern Italy. Ann Chim 93:397–406
Levesque C, Locat J, Leroueil S (2007) Characterization of postglacial sediments of the Saguenay Fjord, Quebec, Canada. In: Characterization and engineering properties of natural soils. Invited paper, Tan, Phoon, Hight et Leroueil (eds). Taylor & Francis, 3:2645–2677
Lisco S, Corselli C, De Giosa F, Mastronuzzi G, Moretti M, Siniscalchi A, Marchese F, Bracchi V, Tessarolo V, Tursi A (2015) Geology of Mar Piccolo, Taranto (southern Italy): the physical basis for remediation of a polluted marine area. J Maps. doi:10.1080/17445647.2014.999136
Liu C, Jay JA, Ika R, Shine JP, Ford TE (2001) Capping efficiency for metal-contaminated marine sediment under conditions of submarine groundwater discharge. Environ Sci Technol 35:2334–2340
Locat J, Lee HJ, Kayen R, Israel K, Savoye MC, Boulanger E (2002) Shear strength development with burial in Eel River Margin Slope sediments. Mar Georesour Geotechnol 20:111–135
Martin F, Konrad J M, Locat J, Locat P, Urgeles R, Lee H (2001) Caractéristiques géotechniques et analyse du potentiel de liquéfaction des sédiments récents et post-glaciaires du fjord du Saguenay, Québec (Canada). Proceedings of the 54th Canadian Geotechnical Conference, Calgary, pp 776–783
Mastronuzzi G (2014) Costruzione del modello geologico, morfologico e sedimentologico del Mar Piccolo; valutazione degli effetti dei flussi di piena; ricostruzione dei bacini morfologici. Technical report, ARPA Puglia-CONISMA
Mastronuzzi G, Sansò P (1998) Morfologia e genesi. In: Mastronuzzi G, Marzo P (eds) Le Isole Cheradi fra natura, leggenda e storia. Fondazione Marittima Ammiraglio Michelagnoli Onlus, Taranto, pp 53–60
Mastronuzzi G, Sansò P (2002) Pleistocene sea level changes, sapping processes and development of valleys network in Apulia region (southern Italy). Geomorphology 46:19–34
Mastronuzzi G, Sansò P (2003) Quaternary coastal morphology and sea level changes. Final Conference-Project IGCP 437 GI2S Coast Coast-Gruppo Informale di Studi Costieri, Otranto/Taranto-Puglia (Italy) 22–28 September 2003, Research Publication 5:34 pp
Meegoda NJ, Ratnaweera P (1994) Compressibility of contaminated fine-grained soils. Geotech Test J 17(1):101–112. doi:10.1520/GTJ10078J
Ministerial Decree n. 468 (2002) Programma nazionale di bonifica e ripristino ambientale. Gazzetta Ufficiale della Repubblica Italiana n. 13 del 2002
Pelletier E, Desrosiers G, Locat J, Mucci A, Tremblay H (2003) The origin and behaviour of a flood capping layer deposited on contaminated sediments of the Saguenay Fjord (Quebec). In: Contaminated sediments: characterization, evaluation, mitigation/restoration, and management strategy performance, Locat J, Galvez Cloutier R, Chaney R, Demars K, (eds). ASTM STP 1442:87–101
Perret D (1995) Diagenèse mécanique précoce des sédiments fins du fjord du Saguenay. PhD thesis. Laval University
Perret D, Locat J, Leroueil S (1995) Strength development with burial in fine-grained sediments from the Saguenay Fjord, Quebec. Can Geotech J 32(2):247–262
Petronio BM, Cardellicchio N, Calace N, Pietroletti M, Pietrantonio M, Caliandro L (2012) Spatial and temporal heavy metal concentration (Cu, Pb, Zn, Hg, Fe, Mn, Hg) in sediments of the Mar Piccolo in Taranto. Water Air Soil Pollut. doi:10.1007/s11270-011-0908-4
Ricchetti G, Ciaranfi N, Luperto Sinni E, Mongelli F, Pieri P (1988) Geodinamica ed evoluzione sedimentaria e tettonica dell'Avampaese Apulo. Mem Soc Geol Ital 41:57–82
Robba E (1969) Il Plio-Pleistocene della zona di Taranto. Riv Ital Paleontol Stratigr 75(3):605–672
Rolling MP (2000) Geotechnical considerations in contained aquatic disposal design. DOER Technical notes collection (ERDC TN-DOER-N5), US Army Engineer Research and Development Center, Vicksburg, MS. www.wes.army.mil/el/dots/doer
Roscoe KH, Schofield AN, Wroth CP (1958) On the yielding of soils. Geotechnique 8(1):22–53
Santamarina JC, Klein KA, Palomino A, Guimaraes MS (2001) Micro-Scale aspects of chemical–mechanical coupling: interparticle forces and fabric. Chemo-mechanical coupling in clays—from nano-scale to engineering applications. Proceedings of the Workshop, Maratea, pp 28–30 June 2001, C. Di Maio, T. Hueckel, and B. Loret, (eds), Balkema, Rotterdam, pp 47–64
Schofield AN, Wroth CP (1968) Critical state soil mechanics. McGraw-Hill, London
Skempton AW (1970) The consolidation of clays by gravitational compaction. Q J Geol Soc 125:373–411
Terzaghi K (1923) Die Berechnung der Durchlassigkeitsziffer des Tones aus dem Verlauf der Hydrodynamischen Spannungserscheinungen Akademie der Wissenschaften in Wien. Mathematisch-Naturwissen-Schaftliche Klasse, Sitzungsberichte, Abteilung IIa 132(3–4):125–138
Tropeano M, Sabato L, Pieri P (2002) Filling and cannibalization of a foredeep: The Bradanic Trough, southern Italy. In: Jones S J &

Frostick L E (eds) Sediment flux to basins: causes, controls and consequences. Geological Society London: Spec Publ 191:55–79
Tursi A, Mastrototaro F (2013) Mappatura biocenotica del Mar Piccolo di Taranto tramite l'utilizzo di ROV e telecamera subacquea trainata sul fondo nonché mediante ispezione subacquea. Technical report, ARPA Puglia – CONISMA
USEPA (2005) Contaminated sediment remediation guidance for hazardous waste sites. https://clu-in.org/download/contaminantfocus/sediments/contaminated-sediment-remediation-EPA-guidance.pdf
Wahid AS, Gajo A, Di Maggio R (2011a) Chemo-mechanical effects in kaolinite. Part 1: prepared samples. Geotechnique 61(6):439–447. doi:10.1680/geot.8.P067
Wahid AS, Gajo A, Di Maggio R (2011b) Chemo-mechanical effects in kaolinite. Part 2: exposed samples and chemical and phase analyses. Geotechnique 61(6):449–457. doi:10.1680/geot.8.P068
Zaitlin BA, Dalrymple RW, Boyd R (1994) The stratigraphic organisation of incised valley systems associated with relative sea-level change. In: Dalrymple RW, Boyd RJ and Zaitlin BA (eds) Incised-valley systems: origin and sedimentary sequences. SEPM Spec Publ 51:45–60